Available online at www.sciencedirect.com
SCIENCE DIRECT®
Journal of Photochemistry and Photobiology A: Chemistry 171 (2005) 281–290
Journal of Photochemistry and Photobiology A:Chemistry
www.elsevier.com/locate/jphotochem

Excited state prototropism in 2-aminonicotinic acid: effect of solvents and acid–base concentrations

Manoj K. Nayak, Sneh K. Dogra*

Department of Chemistry, Indian Institute of Technology Kanpur, Kanpur 208016, India

Received 22 April 2004; accepted 9 September 2004
Available online 8 December 2004

Abstract

Absorption, fluorescence excitation and fluorescence spectroscopy combined with time-dependent spectrofluorimetry have been used to study the effect of solvents and acid–base concentration on the spectral characteristics of 2-aminonicotinic acid (2-ANA). The 2-ANA exists as a molecular species in non-polar and polar aprotic solvents and zwitterion (ZI-1) in polar protic solvents. Dual emission is observed from ZI and the monoanion (MA) of 2-ANA, suggesting that excited state intramolecular proton transfer (ESIPT) is observed from the amino proton to the carbonyl oxygen, followed by structural reorganization. Single normal Stokes shifted fluorescence is observed from the monocation (MC) of 2-ANA, indicating that the carboxylate ion is more effective than –COOH group in ESIPT process. The dication (DC1) is formed by the protonation of =N– and >C=O moieties and dianion by deprotonation of $-NH_2$ and –COOH groups. Electronic molecular structure calculations were performed on each species using semi-empirical quantum mechanical AM1 method and density functional theory (DFT) B3LYP using 6-31G** basis sets with Gaussian 98 to assign the structure to the various species.

Keywords: 2-Aminonicotinic acid; Absorption spectrum; Fluorescence spectrum; Dual fluorescence; ESIPT; Prototropic reactions

1. Introduction

Tramer [1,2], Mataga [3], and Plotnikov and Komarov [5] have shown that 2-amino benzoic acid (2-ABA), 2-*N*-methylamino- and 2-*N*,*N*′-dimethylamino benzoic acid (2-MABA, 2-DMABA) are present as the molecular species in inert solvents and as zwitterionic species (ZI) in polar protic solvents. They proposed that intramolecular hydrogen bonding (IHB) between the $-NH_2$ group and the C=O oxygen is absent in the former species and strong IHB exists in ZI as $-COOH\cdots NR_2$. The presence of the above species has been confirmed using infrared, UV/visible absorption spectra and fluorescence spectra. On the other hand, similar studies carried out on 2-amino-3-naphthaoic acid (2-ANpA) and its methyl ester (2-ANpE) [6] have shown the presence of at least two conformers in both the S_0 and S_1 states. Normal Stokes shifted fluorescence bands in 2-ANpA were assigned to a conformer showing the presence of IHB between an amino proton and the hydroxyl oxygen atom. The large Stokes shifted fluorescence band was assigned to a tautomeric species formed by ESIPT from the amino group to carbonyl oxygen followed by structural rearrangements.

The present study on 2-ANA was carried out to confirm the following points: (i) The effect of solvents on the spectral characteristics of 2-ANA was studied to find out the nature of the excited species. (ii) It has been established that acidity of $-NH_2$ group increases if an electron-withdrawing group is present *ortho* to the $-NH_2$ group [7] or one of the hydrogen atoms is replaced by an electron-withdrawing group [8–11]. The ESIPT rate is enhanced in such molecules if IHB is present in S_0 state with the basic center. In 2-ANA, the pyridine nitrogen and the –COOH group are present *ortho* to the $-NH_2$ group and thus, one may expect ESIPT behaviour. (iii) In 2-aminopyridine (2-AP) [12–14], the =N– atom is more basic than the $-NH_2$ nitrogen atom and if ZI is formed, it will be, most probably, by the protonation of =N– atom

* Corresponding author. Tel.: +91 512 597163; fax: +91 512 590007.
E-mail address: skdogra@iitk.ac.in (S.K. Dogra).

1010-6030/$ – see front matter © 2004 Elsevier B.V. All rights reserved.
doi:10.1016/j.jphotochem.2004.09.017

rather than $-NH_2$ group. In ZI structure, acidity of $-NH_2$ will be increased due to the presence of $=NH^+-$ and $-COO^-$ moieties *ortho* to $-NH_2$ group. Thus, one would expect the enhancement in the rate of ESIPT process and fluorescence intensity of the tautomer band. In order to verifying the above points, absorption, fluorescence excitation and fluorescence spectroscopy combined with time-dependent spetrofluorimetry have been carried out. Electronic molecular structure calculations, using semi-empirical quantum mechanical AM1 method and DFT calculations using 6-31G** basis set and Gaussian 98 program, were performed to assign the proper species. Effects of acid–base concentrations on the absorption, fluorescence excitation and fluorescence spectra were studied in the ground (S_0) and excited (S_1) states. pK_a values were determined for various prototropic reactions and discussed.

2. Materials and methods

The 2-ANA was obtained from Aldrich Chemical Company (U.K.) and was purified by repeated crystallization from methanol. Purity of the compound was confirmed by spectroscopic techniques. Solvents used were either of spectroscopic grade or HPLC grade from E. Merck and were used as such. Spurious emission for each solvent was checked by exciting at the same wavelengths that were used for the fluorophore solution in that solvent. Triply distilled water was used for preparing the aqueous solutions.

Due to poor solubility of 2-ANA in all the solvents, saturated solutions were prepared in each solvent, filtered to remove suspended particles and diluted to such an extent that the absorbance at long wavelength (LW) absorption band maximum is less than 0.1. Instruments used to record absorption and fluorescence spectra and to measure lifetimes are the same as described in our recent paper [15,16]. Hammett's acidity scale (H_0) [17] was used for H_2SO_4–water mixtures for pH < 1 and Yagil's basicity scale (H_-) [18] was used for NaOH–water mixtures for pH > 13. Fluorescence quantum yield (Φ_f) was measured from solutions having absorbance less than 0.1 using quinine sulphate in 1 N H_2SO_4 as reference [19] ($\Phi_f = 0.55$).

3. Theoretical calculations

Scheme 1 depicts various amino rotamers (2-ANA-1, 2-ANA-2), tautomer (2-ANA-T) and imino rotamers (2-INA-1, 2-INA-2). AM1 semi-empirical quantum mechanical calculations (QCMP 137, MOPAC 6/PC) [20] were carried out to get various parameters for the fully optimized geometries of all the species in S_0 state and also in S_1 state after taking into account the configuration interactions (CI = 5 in MOPAC, 100 configurations). Total energy relative to the most stable species (E), heats of formation (ΔH_f) and dipole moment (μ) are compiled in Table 1. Transition absorption energies (ΔE_{ij}) were calculated using CNDO/S-CI method, as suggested by Delbene and Jaffe [21] and Kumar and Mishra [22] and described in our recent publication [15]. Long wavelength (LW) transition for each species is compiled in Table 1. Absorption and emission energy for the first transition were also obtained

Table 1
Calculated parameters of different rotamers/isomers of 2-ANA in S_0 and S_1 states

Characteristics	2-ANA-1	2-ANA-2	2-ANA-T	2-INA-1	2-INA-2
S_0 state					
AM1 method					
ΔH_f (kCal mol^{-1})	−60.5	−58.1	−24.3	−41.5	−40.2
E (kJ mol^{-1})	0	9.8	151.7	79.3	84.9
E_{sol} (kJ mol^{-1})	0	7.0	134.5	52.9	69.9
$\mu_{g\ (D)}$	1.0	1.8	3.1	4.5	3.5
DFT method					
E (kJ mol^{-1})	0	12.17	118.2	74.7	79.8
$\mu_{g\ (D)}$	0.9	1.71	2.7	4.39	2.83
S_1 state					
AM1 method					
E (kJ mol^{-1})	19.0	34.9	126.4	42.8	0.0
E_{sol} (kJ mol^{-1})	41.8	45.7	126.5	18.2	0.0
$\mu_{e\ (D)}$	1.2	3.2	3.6	6.0	4.3
Transition energies (nm)					
Absorption ($S_0 - S_1$)					
Single point	373	365	396	432	426
CNDO/S-CI	309	302	353	345	342
TD (DFT)	310	303	371	392	385
Emission ($S_1 - S_0$)					
AM1 method					
Single point	395	385	678	514	1048

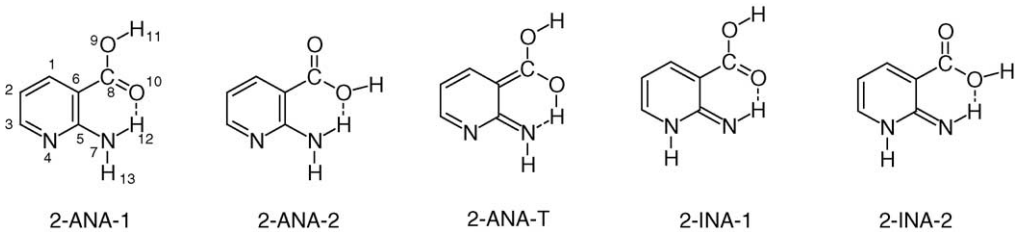

Scheme 1.

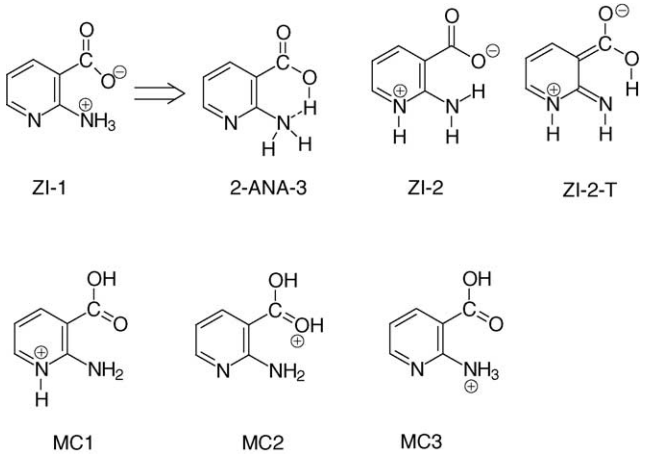

Scheme 2.

by standard single point calculations using AM1 method and by taking the geometry of the respective species in S_0 and S_1 states, respectively. This procedure gives Franck Condon state energies to the respective S_0 and S_1 states. These values also compiled in Table 1.

Similarly, Schemes 2 and 3 depicts the ZI (ZI-1, ZI-2 and ZI-2-T), monocations (MC1, MC2, and MC3) and dications (DC1, DC2 and DC3), respectively. Tables 2–4 give the calculated parameters for the respective species. The electronic structure calculations were also performed on each species, as mentioned in Schemes 1–3, using Gaussian 98 program [23]. The geometry optimization was performed on each species of 2-ANA in S_0 state using DFT [24,25] B3LYP with 6-31G** basis set [23,26]. The geometry of these stationary points on S_1 state was calculated using configuration interaction singles (CIS) [24,27] theory with 6-31G** basis sets. Time-dependent (TD) [28,29] DFT B3LYP was also used to calculate the excited state energies at calculated stationary point geometry in S_0 and S_1 states. Relevant data are compiled in Tables 1–4.

Dipolar solvation energies for different species were calculated using the following expression based on Onsager's theory [30]:

$$\Delta E_{\mathrm{sol}} = -\left(\frac{\mu^2}{a^3}\right) f(D)$$

where $f(D) = (D-1)/(2D+1)$, D is dielectric constant of the solvent, μ dipole moment in the respective state and 'a' the Onsager's cavity radius. Value of 'a' has been calculated by taking 40% of the maximum length of the molecule [31], and it is 0.28 nm. Total energies including solvation energy of each species are compiled in respective tables.

Scheme 3.

Table 2
Calculated parameters of zwitterions and monoanion and their tautomeric structures of 2-ANA in S_0 and S_1 states

Parameters	2-ANA-1	ZI-1/2-ANA-3	ZI-2	ZI-2-T	MA	MA-T
S_0 state						
AM1 method						
ΔH_f (kCal mol^{-1})	−60.5	−48.0	−16.4	−36.2	−82.4	−80.2
E (kJ mol^{-1})	0	52.4	183.6	101.6	0	9.2
E_{sol} (kJ mol^{-1})	183.3	194.7	0	164.8	0	109.8
$\mu_{g\ (D)}$	1.0	4.7	13.7	8.1	7.7	2.8
DFT method						
E (kJ mol^{-1})	0	36.5	68.5	68.5	0	16
$\mu_{g\ (D)}$	0.9	3.1	12.9	8.7	5.99	3.67
S_1 state						
AM1 method						
ΔH_f (kCal mol^{-1})	14.3	42.2	26.7	33.0		
E (kJ mol^{-1})	0.0	115.5	65.5	78.3	33.6	0
E_{sol} (kJ mol^{-1})	114.2	192.4	96.5	0.0	43.2	0
$\mu_{e\ (D)}$	1.2	4.5	6.7	10.3	2.0	3.0
Transition energies (nm)						
Absorption ($S_0 - S_1$)						
Single point	373	293	541	378	325	445
CNDO/S-CI	309	307	506	337	357	360
TD (DFT)	310	281	329.7	–	332	352
Emission ($S_1 - S_0$)						
Single point	395	312	801	472	727	542

Table 3
Calculated parameters of the monocations of 2-ANA in S_0 and S_1 states

Characteristics	MC1	MC2	MC3
S_0 state			
AM1 method			
ΔH_f (kCal mol^{-1})	90.7	115.0	101.5
E (kJ mol^{-1})	0.0	101.6	44.7
E_{sol} (kJ mol^{-1})	0.0	165.1	86.7
$\mu_{g\ (D)}$	6.8	0.9	4.1
DFT method			
E (kJ mol^{-1})	0.0	99.0	59.9
$\mu_{g\ (D)}$	5.9	2.23	3.24
S_1 state			
AM1 method			
E (kJ mol^{-1})	0.0	37.0	104.4
E_{sol} (kJ mol^{-1})	0.0	94.4	141.5
$\mu_{e\ (D)}$	6.59	0.71	3.97
Transition energies (nm)			
Absorption ($S_0 - S_1$)			
Single point	316	432	356
CNDO/S-CI	309	330	344
TD (DFT)	262	341	290
Emission ($S_1 - S_0$)			
Single point	385	532	340

Table 4
Calculated parameters of the dications of 2-ANA in S_0 and S_1 states

Parameters	DC1	DC2	DC3
S_0 state			
AM1 method			
ΔH_f (kCal mol^{-1})	347.0	364.3	363.7
E (kJ mol^{-1})	0.0	72.7	70.0
E_{sol} (kJ mol^{-1})	56.6	117.7	0.0
$\mu_{g\ (D)}$	2.5	3.9	10.1
DFT method			
E (kJ mol^{-1})	0.0	74.8	–
$\mu_{g\ (D)}$	4.24	3.62	–
S_1 state			
AM1 method			
E (kJ mol^{-1})	0.0	68.9	211.5
E_{sol} (kJ mol^{-1})	0.0	64.5	146.3
$\mu_{e\ (D)}$	3.1	3.6	7.0
Transition energies (nm)			
Absorption ($S_0 - S_1$)			
Single point	353	373	275
CNDO/S-CI	298	297	360
TD (DFT)	248	342	–
Emission ($S_1 - S_0$)			
Single point	425	508	327

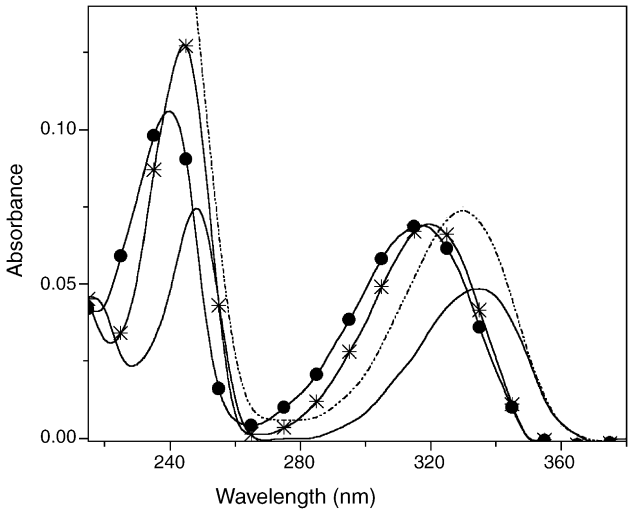

Fig. 1. Absorption spectrum of 2-ANA in some selected solvents: (—): dioxane; (- - -): acetonitrile; (—✳—): methanol; (●): water, pH, 6.4.

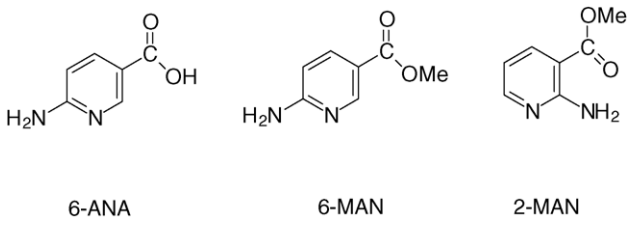

Scheme 4.

4. Results

4.1. Effect of solvents

4.1.1. Absorption spectrum

Fig. 1 depicts the absorption spectrum of 2-ANA in some selected solvents and Table 5 depicts the absorption band maximum (λ^{ab}_{max}) in different solvents. Molecular extinction coefficients in different solvents could not be determined as 2-ANA is only partially soluble in these solvents except water. Similar to methyl 2-aminonicotinate (2-MAN, Scheme 4) [32], two absorption bands are observed in each solvent. On the other hand in case of 6-aminonicotinic acid 6-ANA (Scheme 4) [33], only one λ^{ab}_{max} was observed in polar aprotic solvents. λ^{ab}_{max} of 2-ANA in all the solvents are slightly blue shifted as compared to 2-MAN, and this could be due to the presence of methyl group in the ester group. On acidifying acetonitrile, methanol and water at pH 4, both the λ^{ab}_{max} in acetonitrile are blue shifted, whereas in methanol and water, LW λ^{ab}_{max} is blue shifted by ∼5 nm and short wavelength (SW) λ^{ab}_{max} nearly remains unchanged. This suggests that the species of 2-ANA present in polar aprotic solvent is different than present in polar protic ones. No further change is observed in these two non-aqueous solvents with further increase of acid concentration upto 1 M. Unlike 6-ANA and

Table 5
Absorption band maximum (λ^{ab}_{max}, nm), fluorescence band maximum (λ^{f}_{max}, nm), fluorescence quantum yield (Φ_f) and lifetime (τ, ns), radiative (k_r, 10^7 s^{-1}) and non-radiative (k_{nr}, 10^7 s^{-1}) rate constants of 2-ANA in different solvents

No.	Solvent	λ^{ab}_{max} (nm) (log ε max)		λ^{f}_{max} (nm)		Φ_f^{SW}	Φ_f^{LW}	τ_{SW} (ns)	τ_{LW} (ns)	k_r	k_{nr}
1	Dioxane	248.5	335	382	–	0.58	–	7.4	–	7.84	5.67
2	Ethyl acetate	252	330	380	–	0.48	–	6.1		7.87	8.53
3	Acetonitrile	248	330	381	–	0.50	–	6.7		7.46	7.46
4	Acetonitrile + 10^{-3} M H_2SO_4	243	326	384	–	–	–	–	–	–	–
5	Methanol	244	320	383	485	0.026	0.024	7.1	1.52		
6	Methanol + 10^{-3} M H_2SO_4	244	325	385	–	–	–	–	–	–	–
7	Water pH = 6.4	240 (3.982)	318 (3.838)	384	489	0.011	0.022	–	–	–	–
8	Water pH = 3.6	241 (4.045)	320 (3.892)	390	490	0.002	0.017	7.15	0.6	–	–
9	Water pH = 9.0	243 (4.000)	315 (3.748)	382	486	0.056	0.032	1.33	1.57	–	–
10	Water H_- = 16.0	244 (4.053)	316 (3.756)	–	505	–	0.0075	–	0.53	1.41	187.2
11	Water pH = 0.0	244 (4.083)	325 (3.945)	386	491	0.01	0.0037	–	–	–	–
12	Water H_0 = −5.0	244 (4.124)	325 (4.005)	382	–	0.373	–	6.75	–	5.52	9.29
13	Water H_0 = −10.0	246 (3.995)	329 (3.963)	400	–	0.58	–	8.05	–	7.2	5.22

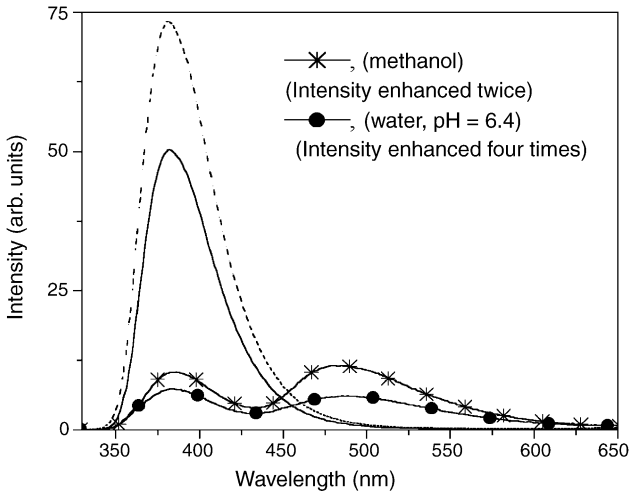

Fig. 2. Fluorescence spectrum of 2-ANA in some selected solvents: (—): dioxane; (- - -): acetonitrile; (—✳—): methanol (intensity enhanced twice); (●): water; pH, 6.4 (intensity enhanced four times).

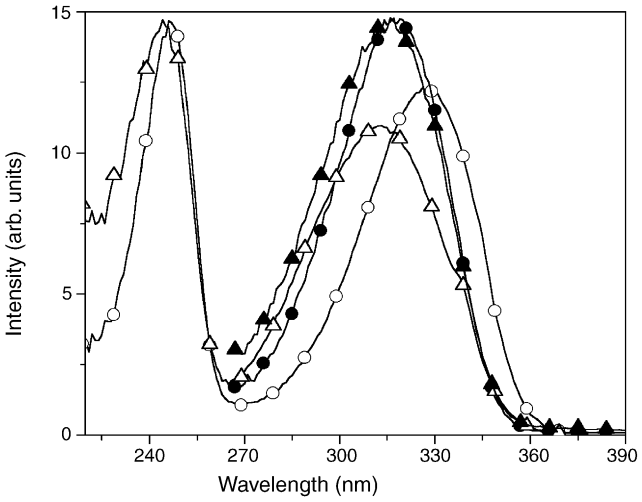

Fig. 3. Normalized fluorescence excitation spectrum of 2-ANA in methanol and water (pH = 6.4): (◯): λ_{em} = 385 nm; (●): λ_{em} = 530 nm, methanol; (Δ): λ_{em} = 385 nm, (▲): λ_{em} = 530 nm, water.

2-MAN, λ^{ab}_{max} of 2-ANA is blue shifted with increase in the polarity and protic nature of solvents. As mentioned above, in polar protic solvents, 2-ANA seems to be partially dissociated and dissociation increases with increase of protic nature (see later) and thus, absorption spectrum in these solvents cannot be assigned to neutral species. Full width at half the maximum height (FWHM) of the LW absorption band increases with increase of solvent polarity. This could be either due to dissociation of neutral 2-ANA or due to net solvent interactions.

4.1.2. Fluorescence spectrum

Fig. 2 depicts the fluorescence spectrum of 2-ANA in some selected solvents and relevant data are compiled in Table 5. In less polar aprotic solvents, only one normal Stokes shifted fluorescence band is observed at ∼380 nm, which is red shifted to that in 6-ANA [33] but at the similar position as observed in 2-MAN [32]. Φ_f and FWHM of the emission band of 2-ANA in dioxane, ethylacetate and acetonitrile are invariant to λ_{exc} and solvent polarity. In polar protic solvents, e.g. methanol and water (pH 6.4), dual emission is observed at all the λ_{exc} used (300, 320 and 340 nm). SW λ^{f}_{max} and FWHM are not sensitive to λ_{exc} and solvent, but its Φ_f in methanol decreases with increase of λ_{exc}, whereas it does not change in water. On the other hand, LW λ^{f}_{max} is red shifted by 4 nm on going from methanol to water (pH = .4). In both of these solvents, λ^{f}_{max}, Φ_f and FWHM of LW emission are not functions of λ_{exc}. This suggests that emission in each case is occurring from the most relaxed state, and this is expected as the solvent relaxation times of the solvents used are smaller than the lifetimes of the fluorophore. Further, λ^{f}_{max} and Φ_f of SW emission band of 2-ANA in protic solvents is quite different from those of 2-MAN [32], suggesting that species of 2-ANA and 2-MAN involved in these solvents are quite different from each other.

4.1.3. Fluorescence excitation spectrum

Fluorescence excitation spectrum of 2-ANA recorded in dioxane, ethyl acetate and acetonitrile at different λ_{em} resemble with each other and also with the absorption spectrum in each solvent, suggesting that there is only one species in S_0 state and the absorbing and emitting species are the same. In case of methanol as solvent, SW fluorescence excitation peak is at the same wavelength at each λ_{em} in the range of 365–530 nm, whereas LW fluorescence excitation peaks are at 327 and 319 nm when monitored in the range of 365–420 nm and 470–530 nm, respectively. Similar behaviour is also observed for 2-ANA in case of water as solvent except that LW fluorescence excitation peaks are at 313 and 316 nm when monitored at λ_{em} between 365–420 nm and between 470–530 nm, respectively (Fig. 3). In other words, in both the solvents, two species are present in S_0 state with different LW fluorescence excitation spectra. Both these LW fluorescence excitation bands are blue shifted with increase in polarity and protic nature of the solvents, but the blue shift observed in the fluorescence excitation band maximum corresponding to SW emission is much larger (327–313 nm) than that observed for LW emission (319–316 nm). Thus, absorption spectrum of 2-ANA in methanol and water are the composite of the absorption spectra of two ground state species. In all the solvents, the LW fluorescence excitation spectra and SW fluorescence spectra overlap with each other, indicating that ∼384 nm emission is a normal fluorescence band.

4.1.4. Excited state lifetimes

Excited state lifetimes of 2-ANA were measured by exciting at 337 nm and using λ_{em} as the band maximum in the respective solvents. In polar protic solvents, 311 nm was also used as λ_{exc} and λ_{em} were 380 and 480 nm. In polar aprotic solvents, fluorescence decay profile followed a single exponential with $\chi^2 = 1 \pm 0.1$ and good autocorrelation function. In methanol as solvent, fluorescence decay profile

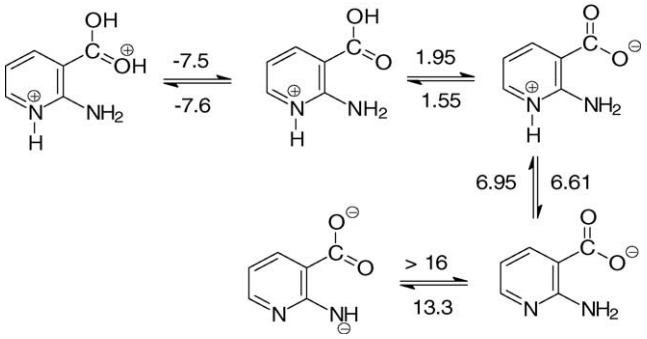

Scheme 5.

followed double exponential at $\lambda_{exc} = 311$ and 337 nm and $\lambda_{em} = 480$ nm, whereas a single exponential is observed for $\lambda_{em} = 380$ nm. On the other hand, single exponential decay is observed at both λ_{exc} and λ_{em} in water. Relevant data are compiled in Table 5.

4.2. Effect of acid–base concentration

4.2.1. Aqueous medium

Hardly any change is observed in LW λ^{ab}_{max} of 2-ANA in the pH/H_- range of 8–16, whereas the absorbance of SW λ^{ab}_{max} increases with an increase in base concentration without any change in λ^{ab}_{max}. Thus, the pK_a value for the MA–DA equilibrium could not be determined in the S_0 state. With a decrease of pH from 9, LW λ^{ab}_{max} shifts to the red from 315 to 320 nm with an increase in absorbance, whereas SW λ^{ab}_{max} shifts to the blue by 3 nm. The species so formed at pH 3.6 could be zwitterion (ZI) and pK_a value evaluated using absorbance for ZI–MA equilibrium is found to be 6.6. With further increase of acid concentration, both the absorption bands are red shifted by 4–5 nm with slight increase in the absorbance and having isosbestic point at 315 nm. The change in the absorption spectrum may be assigned to the formation of MC by protonating carboxylate ion. Presence of isosbestic point depicts the equilibrium between two species and pK_a value for MC–ZI equilibrium is 1.95. With further increase of acid concentration absorbance of both the bands increase by 10–15% upto $H_0 = -5$ without much change in band maxima and then decrease with red shift in both the absorption bands. Similar behaviour is observed in case of amino benzoic acids [2,5] and 6-ANA [33] and 2-MAN [32]. pK_a values obtained are approximate ones and given on the top of arrows depicting the various equilibria in Scheme 5. Absorption spectra of different species are given in Fig. 4.

Unlike absorption spectrum of 2-ANA but similar to 2-MAN, a very weak fluorescence broad band appears at 505 nm and at H_- 16. With decrease of pH, an intense dual fluorescence band system appears at 382 and 486 nm at the expanse of 505 nm emission band. With decrease of pH, the dual fluorescence system is still retained even at pH 3.6. The only difference is that in MA, the fluorescence intensity of SW band is larger than that of LW emission, whereas in case of ZI, the fluorescence intensity of SW emission band is smaller than that of LW emission band. Of course, the fluorescence intensity of both the bands of ZI is smaller than those of MA. λ^{f}_{max} of dual emission are red shifted by 4 nm in each case in going from MA to ZI. With increase of acid concentration, the dual emission band of ZI is replaced by a single emission band at 386 nm, blue shifted by 4 nm with respect to the SW emission band of ZI, possessing an isoemissive point at ~440 nm, just like an isosbestic point in the absorption spectra. This suggests the presence of only two species in S_1 state. With further increase in acid concentration, the fluorescence spectrum is slightly blue shifted by 4 nm with drastic increase in fluorescence intensity up to $H_0 = -5$, but with further increase of acid concentration, the emission spectrum is red shifted to 400 nm with increase of Φ_f. Fig. 5 depicts the flourescence spectra of different ionic species.

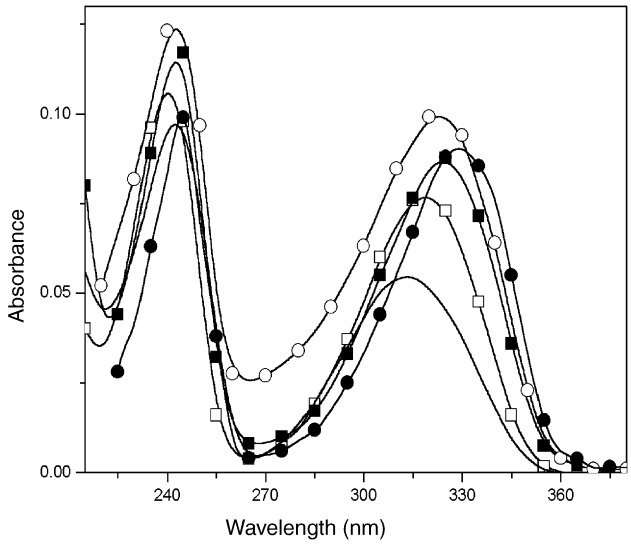

Fig. 4. Absorption spectrum of different ionic species of 2-ANA: (●): $H_0 = -10.0$; (◯): $H_0 = -5.0$; (■): pH = 0.0; (□): pH = 3.6; (—): pH = 10.5; [2-ANA] = 1×10^{-5} M.

Fluorescence excitation spectra recorded at pH = 10 and H_- 16 in the range 365–540 nm, covering the emission of DA and dual emission of MA, are similar to each other and to absorption spectra. This suggests that the precursor for the MA and DA species in S_0 state is the same. Similarly, the dual emission of MA also arises from the same ground state species and appearance of dual emission in MA is an excited state phenomenon. This is manifested by the fact that the fluorescence intensity ratios of SW to LW emission bands remain same at each pH in the range of pH 8 to H_- 16. Single exponential in the fluorescence decay profile with $\tau = 0.53$ ns at H_- 16 suggests the presence of only one DA species and it is different from those observed at pH 10.5 and at $\lambda_{em} = 380$ (1.3 ns) and $\lambda_{em} = 480$ nm (1.6 ns). Lifetimes observed at these wavelengths and pH = 10.5 are independent of λ_{exc}. This suggests that although the species formed in S_1 state are different, but possesses the same precursor in S_0 state.

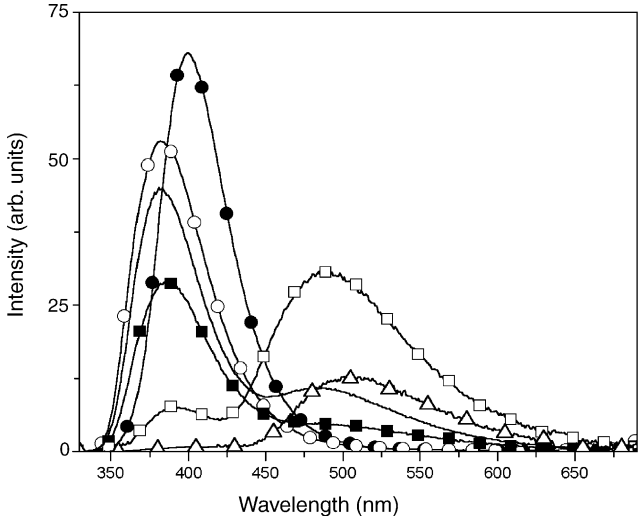

Fig. 5. Fluorescence spectrum of different ionic species of 2-ANA: (●): $H_0 = -10.0$; (○): $H_0 = -5.0$; (■): pH = 0.0 (intensity enhanced 20 times); (□): pH = 4.5 (intensity enhanced 30 times); (—): pH = 10.5 (intensity enhanced 10 times); (Δ): $H_- = 16$ (intensity enhanced 40 times). At $\lambda_{ex} = 320$ nm and [2-ANA] = 1×10^{-5} M.

As mentioned earlier and similar to that observed in case of methanol fluorescence excitation spectra recorded at pH 3.6 and at different λ_{em} do not match with absorption spectrum. Fluorescence excitation spectrum recorded at λ_{em} 370–420 nm is slightly red shifted (320 nm) than that recorded at λ_{em} 470–530 nm (317 nm), suggesting that each emission band may be due to different ground state species. This is supported by different lifetimes observed at 380 nm ($\tau = 7.15$ ns) and at 480 nm (0.6 ns). This also suggests that the equilibrium between the two species in S_1 state is not established. The fluorescence excitation spectrum at H_0 of 0, −5 and −10 at different λ_{em} resemble with each other and also with absorption spectrum of each species. This suggests that there is only one species at each acid concentration in S_0 state and the absorbing and emitting states are the same. This is also reflected by single exponential, observed in the fluorescence decay profile of each species.

4.2.2. Non-aqueous medium

Both the absorption band systems are blue shifted by 4 and 5 nm in acetonitrile containing 10^{-3} M H_2SO_4, followed by no effect with further increase of H_2SO_4 up to 1 M. On the other hand, LW λ^{ab}_{max} is red shifted by 5 nm at 10^{-3} M H_2SO_4 in methanol, with no change in SW λ^{ab}_{max}. Similar to acetonitrile, no further change is noticed in λ^{ab}_{max} on further addition of H_2SO_4 in methanol. Contrary to absorption spectrum, fluorescence spectrum is red shifted by 5 nm in acetonitrile at 10^{-3} M H_2SO_4, followed by no change either in λ^{f}_{max} or intensity. Dual emission band in methanol reduces to single normal emission at 385 nm, red shifted by 2 nm as compared to SW λ^{f}_{max} in methanol without H_2SO_4.

5. Discussions

5.1. Assignment of species

As observed in case of 2-AP and other substituted 2-AP [34–40], present results also suggest that imino forms of 2-ANA (2-INA-1 and 2-INA-2) are highly unstable as compared to the most stable form of 2-ANA-1 by 79.3, 52.9 and 84.9, 69.9 kJ mol^{-1} in S_0 state both under isolated conditions and when dipolar solvation energies are included. Similar to 2-AP [39] and 2-MAN [32], the activation energy barrier for the amino-imino equilibrium is also expected to be very large in S_0 and S_1 states. Heats of formation and DFT calculations also support the above results in S_0 state (Table 1). Similar to the results of 2-AP in S_1 state [39], taking into account configuration interactions in S_1 state, AM1 calculations also show that 2-INA-2 is the most stable species under isolated conditions and including dipolar solvation energies. Considering the similar behavior as observed in 2-AP, it may also be concluded that imino forms of 2-ANA are not possible in S_0 and S_1 states.

Considering the results of AM1 calculations 2-ANA-T can also be rejected as it is unstable both in S_0 and S_1 states by 151.7 and 107.4 kJ mol^{-1} under isolated conditions and by 134.5 and 84.7 kJ mol^{-1} when dipolar solvation energy is included as compared to 2-ANA-1. Similar results are also obtained from ΔH_f and DFT calculations. Further, the activation barrier for IPT in S_1 state decreases to 119.9 kJ mol^{-1} from 156 kJ mol^{-1} in S_0 state. Still it is quite large. Results of Table 1 also suggest that 2-ANA-1 is more stable than 2-ANA-2 in S_0 state by 9.8 kJ mol^{-1} under isolated conditions and 7.0 kJ mol^{-1} when dipolar solvation energies are included. On the other hand in S_1 state, stability of 2-ANA-1 increases to 15.9 kJ mol^{-1} under isolated conditions and decreases to 4 kJ mol^{-1} when dipolar solvation energy is included. These data also reflect the relative strength of IHB between amino proton and carbonyl group and between amino proton and –OH oxygen atom of –COOH group. These results are consistent with the fact that IHB between $-NH_2$ proton and >C=O oxygen atom is stronger than that between $-NH_2$ proton and –OH oxygen atom. Based on activation barrier energy data (24.9 and 47.4 kJ mol^{-1} in S_0 and S_1 states, respectively) for the conversion of 2-ANA-1 to 2-ANA-2, it can be concluded that inter conversion of 2-ANA-1 to 2-ANA-2 will be less feasible in S_1 state in comparison to that in S_0 state, which is also prohibited at room temperature.

Having established that 2-ANA-1 is the only molecular species present, both in S_0 and S_1 states, we would like to compare the stability of 2-ANA-1 as compared to ZI-1 and ZI-2. Results of Table 2 have shown that the optimized structure of ZI-1 is not the charged neutral species, but it is a neutral species where –COOH proton is intramolecularly hydrogen bonded to $-NH_2$ lone pair ($-COOH\cdots NH_2$). Similar results have also been observed by Tramer for 2-ABA [1,2]. The species may thus be called as 2-ANA-3. Heats of formation, total energy obtained by AM1 method and DFT

calculations have shown that 2-ANA-1 is stable species under isolated conditions as compared to ZI-1/(2-ANA-3) and ZI-2 by 52.4 and 183.6 kJ mol^{-1}, respectively in S_0 state and by 115.5 and 65.5 kJ mol^{-1} in S_1 state. On the other hand, when dipolar solvation energies in water are included, ZI-2 becomes the most stable species by 183.3 and 194.7 kJ mol^{-1} in S_0 state and by 17.7 and 95.9 kJ mol^{-1} in S_1 state as compared to 2-ANA-1 and ZI-1. In other words, 2-ANA-1 is the species present in less polar medium and ZI-2 in polar protic medium.

After establishing the presence of 2-ANA-1 and ZI-2, the experimental results can be discussed as follows: (i) λ^{ab}_{max} and λ^{f}_{max} of 2-ANA resemble with those of 2-MAN [32] in polar aprotic solvents and are red shifted with respect to 6-ANA and 6-MAN [33]. In 6-ANA and 6-MAN, IHB is absent. This suggests that the red shift observed in the spectral characteristics of 2-ANA is due to IHB. In 2-ANA, IHB can be either between –NH_2 proton and >C=O oxygen/hydroxyl oxygen atom (2-ANA-1, 2-ANA-2) or between acidic proton of –COOH and –NH_2 lone pairs (2-ANA-3), whereas in 2-MAN, IHB can be only between –NH_2 proton and >C=O oxygen. Resemblance of spectral characteristics of 2-ANA and 2-MAN suggests that 2-ANA exists as molecular species (2-ANA-1) in polar aprotic solvents. This seems to be consistent because replacing proton by methyl group in –COOH does not affect the spectral characteristics of the system very much. In other words, spectral assignment of 2-ANA can be explained on the same lines as done for 2-MAN [32]. This is further supported by the single exponential decay, only one normal Stokes shifted fluorescence band and similar fluorescence excitation spectra recorded at different λ_{em}. In protic solvents, no change was observed in λ^{ab}_{max} and λ^{f}_{max} of 2-MAN as compared to polar aprotic solvents. On the other hand, LW λ^{ab}_{max} of 2-ANA was blue shifted at pH 10.5 and 3.6 as compared to that in polar aprotic solvents, suggesting that the species of 2-ANA present at this pH and in this pH range are different from those in aprotic polar solvents. Since 2-ANA contains dissociable proton, it can either lead to MA at pH 10.5 or ZI-2 at pH 3.6 and mixture of both in the pH range of 3.6–10.5. Presence of ZI-2 is supported by the fact that protonation constant of =N– in 2-AP [1–3] and nicotinic acid [41] are 6.75 and 4.72, respectively, whereas that in 2-ABA is 2.55 [5], i.e. =N– atom is the most basic and will be protonated in preference to –NH_2. pK_a value of 6.5 observed in 2-ANA supports the formation of ZI-2.

It has been shown in the earlier paragraph that ESIPT is not possible in 2-ANA in any polar aprotic solvents. Thus, the dual emission observed in methanol and water (pH = 3.6) is due the presence of ZI-2. Although the results of Table 2 show that ZI-2-T is stable than ZI-2 by 82 kJ mol^{-1} under isolated conditions in S_0 state, but both species are highly unstable than 2-ANA-1 under the similar conditions. When dipolar solvation energy is included in S_0 state, ZI-2-T is unstable as compared to ZI-2, which is the most stable species. On the other hand, DFT calculations always lead to ZI-2 as the most stable structure even if we start with ZI-2-T as the starting geometry. Thus, it may be concluded that ZI-2 is the only species present in S_0 state in polar protic solvents. In S_1 state, AM1 calculations suggest that the order of stability of different species under isolated conditions in 2-ANA is 2-ANA-1 > ZI-2 > ZI-2-T, whereas in polar protic solvents, the order of stability is ZI-2-T > ZI-2 > 2-ANA-1. In other words, ESIPT in 2-ANA will not be observed in non-polar solvents and is only feasible in polar protic ones. We could not confirm the former results as 2-ANA is completely insoluble in cyclohexane, but the results in acidified acetonitrile have confirmed the presence of MC1 at 10^{-3} M H_2SO_4, as only one normal Stokes shifted emission was observed at 386 nm. Dual emission observed in water at pH = 3.6 confirms the latter conclusion. On comparing the results with 2-MAN (where IHB is also present between –NH_2 proton and >C=O oxygen) [32] it is concluded that ESIPT in 2-ANA is observed because of the presence of better proton acceptor carboxylate ion (–COO–) than the –COOMe group.

5.2. MC–ZI equilibrium

Three possible MCs (MC1, MC2, and MC3) are depicted in Scheme 2 and relevant data are compiled in Table 3. It is evident from AM1 data that MC1 is more stable than MC2 and MC3 by 101.6 and 44.7 kJ mol^{-1} under isolated conditions and its stability increases to 165 and 86.7 kJ mol^{-1}, respectively when solvation energy is included in S_0 state. Similar conclusion can also be drawn from the results of heats of formation and DFT calculations (Table 3). Results of S_1 state after fully optimizing the geometry of each species and taking into account the configuration interactions, also predict that MC1 is the most stable species as compared to MC2 and MC3 by 37.0 and 104.4 kJ mol^{-1} under isolated conditions and 94.4 and 141.5 kJ mol^{-1}, respectively when dipolar energies are included. All these results suggest that MC1 is the only monocationic species present in S_0 and S_1 states. These conclusions are supported by the following results:

(i) pK_a values for the protonation reaction of 2-AP [12–14] and 2-ABA [1–5] are 6.86 and 2.55, respectively. pK_a value for MC–ZI equilibrium in 2-ANA in the present study is 6.6.

(ii) Protonation of amino group of ZI-2 will lead to blue shift in spectral characteristics and thus should resemble with those of zwitter ion of nicotinic acid or molecular form of nicotinic acid (i. e. 276 nm) [41,42]. Similarly, the protonation of –NH_2 group of 2-ABA leads to the spectral characteristics of benzoic acid and the species so formed is non-fluorescent [5]. In the present case, slight red shift (∼5 nm) observed in λ^{ab}_{max} and blue shift in λ^{f}_{max} (4 nm) at pH = 0 contradicts the above results.

(iii) Spectral absorption and emission transitions predicted by AM1 method for MC1 agree nicely with those observed experimentally. Agreement between the predicted absorption transitions by other methods for MC1 with experimental results is also not that bad.

(iv) λ^{ab}_{max} and λ^{f}_{max} of the MC of 2-ANA agree nicely with that of 2-MAN [32].

(v) Fluorescence excitation spectra monitored at different λ_{em} are similar to each other and resemble with the absorption spectrum. Excited state lifetime could not be determined because of poor Φ_f of MC. Intersection of fluorescence and fluorescence excitation spectra depicts a normal Stokes shifted fluorescence and thus confirms the presence of only one monocation i.e. MC1. pK_a value obtained from fluorimetric titrations suggests that MC–ZI equilibrium is not established in S_1 state and could be due to slower rate of protonation/deprotonation reactions as compared to the radiative decay rates of the conjugate acid–base pair.

5.3. Dication–Monocation equilibrium

Similar to MCs, three DCs can be formed by further protonating the basic centers (DC1, DC2, DC3, Scheme 3). Heats of formation and total energy data depict that DC1 is the most stable species in the S_0 state under isolated conditions and DC3 is the most stable when dipolar solvation energy is included. DFT calculations, under isolated conditions also predict the similar results. It may also be mentioned here that DFT calculations only predict DC1 to be most stable even if we start with DC3 geometry. In S_1 state, after taking into considerations the configuration interactions (CI = 5 in MOPAC, 100 configurations), DC1 is most stable dicationic species. Thus, under all circumstances, DC1 is the only species in S_0 and S_1 states except in polar protic media where DC3 is the species in S_0 state. Spectral characteristics observed for 2-ANA in the acid concentration range of $H_0 = 0$ to -10 are exactly similar to those observed for 2-MAN [32] under the similar conditions. Thus, the prototropic reactions occurring in 2-ANA can be explained on the similar lines, i.e. DC1 is the only dicationic species in this acid range.

5.4. Zwitterion–Monoanion

As established earlier, ZI-2 (Scheme 2) is the stable species in polar protic solvent. MA from this can be formed either deprotonating $=NH^+-$ moiety or $-NH_2$ group. The latter is neglected on the ground that the pK_a value for the deprotonation of $-NH_2$ group is >16 [43–46]. Observed pK_a value of 6.6 in the present case, thus, neglects the deprotonation of $-NH_2$ group at pH = 10.6. Results of Table 2 suggest that the intramolecular proton transfer (IPT) in MA of 2-ANA in S_0 state is not possible as the tautomer (MA-T) so formed from MA is unstable by 9.2 and 109.8 kJ mol^{-1}, respectively under isolated conditions and when solvation energies are included. Further, the activation barrier for IPT in S_0 state is 64.2 kJ mol^{-1}. In other words, formation of MA-T is highly improbable in S_0 state at room temperature. Small blue shift observed in LW λ^{ab}_{max} and SW λ^{f}_{max} in comparison to ZI-2, could be due to strong IHB between $-NH_2$ proton and $-CO_2^-$ moiety. This is also consistent with the results about the order of λ^{ab}_{max} observed for various species as λ^{ab}_{max} (ZI) > λ^{ab}_{max} (MA) > λ^{ab}_{max} (MC) > λ^{ab}_{max} (N) [47]. Dual fluorescence and only one fluorescence excitation band maximum at both the emission suggests the presence of only one species in S_0 state and dual emission is an excited state process, i.e. ESIPT. These results also indicate that IHB between $-NH_2$ proton and $-CO_2^-$ is very strong and is retained even in aqueous medium. The presence of ESIPT reaction is supported by the results of Table 2 that MA-T is highly stable in S_1 state by 33.6 and 43.2 kJ mol^{-1} under isolated conditions and when dipolar solvation energy is included, respectively. The activation barrier energy for IPT in S_1 state also reduces to 43.5 from 64.2 kJ mol^{-1} in S_0 state. Although activation barrier is still large in S_1 state, but it suggests that relatively it becomes feasible in S_1 state in comparison to S_0 state. Similar results are also observed in other systems [48–51]. Single lifetime observed for MA and MA-T confirms the presence of only one kind of species in S_1 state, and equilibrium is not established in S_1 state as the lifetimes for MA and MA-T are different.

DA can only be formed by the deprotonation of $-NH_2$ group and thus, there can be only one species in S_1 state. This is consistent with only one fluorescence band maximum, similarly, fluorescence excitation band recorded at different λ_{em} and single exponential decay observed in the fluorescence decay profile. This is also supported by the fact that $-NH_2$ group becomes stronger acid on excitation to S_1 state [43–46]. In general, species formed by the deprotonation of $-NH_2$ group of aromatic amines is non-fluorescent with few exceptions [52] and the DA so formed from 2-ANA belongs to latter categories. The non-fluorescent nature of MA of aromatic amines has been attributed to the solvent induced fluorescent quenching [53].

The pK^*_a values for both equilibriums were determined using fluorimetric titration method and exciting at the isosbestic point for ZI–MA and λ^{ab}_{max} in the latter case. Value obtained for ZI–MA is the ground state pK_a value, indicating that the ZI–MA prototropic equilibrium is not established in this case and could be due to the shorter lifetimes of the respective conjugate acid–base pairs as compared to the reciprocal rate of deprotonation and protonation rate in S_1 state. Smaller value of pK^*_a for MA–DA equilibrium confirms that $-NH_2$ group becomes stronger acids in S_1 state [43–46].

6. Conclusions

Following conclusions can be drawn from the above study: (i) 2-ANA exists as the amino form both in S_0 and S_1 states. Imino forms are absent. (ii) 2-ANA is present in the molecular neutral form in polar aprotic solvents. (iii) Dual fluorescence is observed from MA, by ESIPT process from $-NH_2$ group to $-COO^-$ moiety followed by structural rearrangement. Both the emission bands possess the same ground state precursor, suggesting that IHB is very strong between $-NH_2$ and

$-COO^-$ moieties even in aqueous medium. Different lifetimes for the two species suggest that equilibrium is not established in S_1 state. (iv) Dual fluorescence observed in case of ZI-2 can also be explained on the same lines. Both these observations, (iii) and (iv) confirm that the acidity of $-NH_2$ group increases due to the presence of electron-withdrawing groups at *ortho* to $-NH_2$ and ESIPT rate is enhanced if the basicity of electron-withdrawing groups is increased. It also suggests that $-COO^-$ moiety is better proton acceptor than –COOMe group. (v) Normal Stokes shifted emission observed in case of MC1 suggests that either the acidity of $-NH_2$ group is not enhanced that much due to the presence of $=NH^+-$ group or IHB in MC1 could be between the lone pair of $-NH_2$ group and proton of –COOH, which does not lead to ESIPT. Similar behaviour is also observed in 2-ABA [1,2].

Acknowledgement

The authors are thankful to the Department of Science and Technology, New Delhi for the financial support to the project number SP/S1/H-07/2000.

References

[1] A. Tramer, J. Mol. Struct. 4 (1969) 313.
[2] A. Tramer, J. Phys. Chem. 74 (1970) 887.
[3] N. Mataga, Bull. Chem. Soc. Jpn. 36 (1963) 654.
[4] V.G. Plotnikov, V.M. Komarov, Spectrosc. Lett. 9 (1976) 265.
[5] D.V.S. Jain, F.S. Nandel, P. Singla, D.J. Kaur, Indian J. Chem. 25A (1986) 15, and other references listed therein.
[6] S. Srivastava, S.K. Dogra, J. Photochem. Photobiol. A: Chem. 46 (1989) 329.
[7] M.M. Balamurali, S.K. Dogra, Chem. Phys. 305 (2004) 95.
[8] P.T. Smith, K.A. Zaklike, K. Thakur, P.F. Barbara, J. Am. Chem. Soc. 113 (1991) 4035.
[9] S. Santra, M. Krishnamoorthy, S.K. Dogra, J. Phys. Chem. 104 (2000) 4761.
[10] S. Santra, M. Krishnamootrhy, S.K. Dogra, Chem. Phys. Lett. 311 (1999) 915.
[11] S. Santra, M. Krishnamoorthy, S.K. Dogra, Chem. Phys. Lett. 327 (2000) 230.
[12] A. Weisstuch, A.C. Testa, J. Phys. Chem. Chem. 72 (1968) 1982.
[13] A.C. Testa, U.P. Wild, J. Phys. Chem. 85 (1981) 2637, and earlier references listed therein.
[14] S.G. Schulman, A.C. Capomacchia, A.K. Riela, Anal. Acta 56 (1971) 91.
[15] G. Krishnamoorthy, S.K. Dogra, J. Org. Chem. 64 (1999) 6566.
[16] M.K. Nayak, S.K. Dogra, J. Photochem. Photobiol. A: Chem. 161 (2004) 169.
[17] M.J. Jorgenson, D.R. Hartter, J. Am. Chem. Soc. 79 (1957) 427.
[18] G. Yagil, J. Phys. Chem. 71 (1967) 1034.
[19] S.R. Meach, D.J. Phillips, J. Photochem. 23 (1983) 193.
[20] M.J.S. Dewar, E.G. Zoeblish, E.F. Healy, J.J.P. Stewart, J. Am. Chem. Soc. 107 (1985) 3092.
[21] J. Delbene, H.H. Jaffe, J. Chem. Phys. 48 (1962) 1807.
[22] A. Kumar, P.C. Mishra, QCPE Bull. 9 (1989) 67.
[23] M. Head-Gorden, E.S. Replogte, J.A. Pople, Gaussian 98, Revision, A.T. Gaussian Inc., Pittsberg, PA, 1998.
[24] A.D. Becke, J. Chem. Phys. 98 (1993) 546.
[25] R.G. Parr, W. Yang, Density Functional Theory of Atoms and Molecules, A.T. Gaussian Inc., Pittsberg, PA, 1998.
[26] G.A. Peterson, M.A. Al-Lahan, J. Chem. Phys. 94 (1991) 6081.
[27] J.B. Foresman, A. Frish, Exploring Chemistry with Electronic Structure Methods, 2nd ed., Gaussian Inc., Pittsberg, PA, 1998.
[28] J.B. Foresman, M. Head-Gorden, J.A. Pople, M.J. Frish, J. Phys. Chem. 96 (1992) 135.
[29] M.E. Casido, G. Jamorski, K.C. Casido, D.R. Salahub, J. Chem. Phys. 108 (1998) 439.
[30] N. Mataga, T. Kubata, Molecular Interactions and Electronic Spectra, Marcel Dekker, New York, 1970.
[31] E. Lippert, Z. Electrochem. 61 (1957) 862.
[32] M.K. Nayak, S.K. Dogra, J. Photochem. Photobiol. A: Chem., in press.
[33] Absorption and fluorescence band maxima of 6-MAN in cyclohexane and water (pH = 8) are at 265 and 324 nm and 274 and 364 nm, respectively of 6-ANA in dioxane, acetonitrile and water (pH = 4.5) are 270 and 338; 270 and 339 nm and 252 and 365 nm.
[34] J. Hager, S.C. Wallace, J. Phys. Chem. 89 (1985) 2637.
[35] K. Konijner, A. Fujimoto, Spectrochim. Acta 42A (1986) 929.
[36] J. Konijner, A.H. Huizer, A.G.O. Verma, J. Chem. Soc. Trans. Faraday 2 (85) (1989) 1539.
[37] A. Fujimoto, K. Inuzuka, Bull. Chem. Soc. Jpn. 64 (1991) 3758.
[38] H. Ishikawa, K. Iwata, H. Hamuguchi, J. Phys. Chem. A 106 (2002) 2305.
[39] B. Kim, C.P. Schick, P.M. Weber, J. Chem. Phys. 103 (1995) 6903.
[40] F. Hung, W. Hu, T. Li, C. Chang, P.T. Chou, J. Phys. Chem. A 107 (2003) 6903.
[41] R.F. Evans, E.F.G. Harington, W. Kynaston, Trans. Faraday Soc. 49 (1953) 1284.
[42] R.F. Green, H.K. Tong, J. Am. Chem. Soc. 78 (1956) 4896.
[43] M. Swaminathan, S.K. Dogra, Can. J. Chem. 61 (1983) 1064.
[44] A.K. Mishra, S.K. Dogra, J. Photochem. 105 (1983) 163.
[45] M. Swaminathan, S.K. Dogra, J. Am. Chem. Soc. 105 (1983) 6223.
[46] R.V. Subbarao, M. Swaminathan, S.K. Dogra, J. Photochem. 34 (1986) 55.
[47] S.G. Schulman, A.C. Capomacchia, B. Tussey, Photochem. Photobiol. 14 (1971) 733.
[48] F. Marquez, I. Zabala, F. Thomas, Anals de Quim. 91 (1995) 647.
[49] S. Maheshwari, A. Chowdhury, N.S. Sathyamurthy, H. Mishra, H.B. Tripathi, M. Panda, J. Chandrasekhar, J. Phys. Chem. 103 (1999) 6257.
[50] P. Purkaystha, N. Chattopadhyay, Phys. Chem. Chem. Phys. 2 (2000) 203.
[51] M.M. Balamurali, S.K. Dogra, J. Photchem. Photobiol. A: Chem. 154 (2002) 81.
[52] A.K. Mishra, M. Swaminathan, S.K. Dogra, J. Photochem. 29 (1985) 87.
[53] R.S. Sarpal, S.K. Dogra, J. Chem. Soc. Trans. Faraday I 88 (1992) 2725.